CONF-950750--48
SAND95-2704C

PBFA II-Z: A 20-MA DRIVER FOR Z-PINCH EXPERIMENTS*

R. B. Spielman, F. Long, T. H. Martin, J. W. Poukey, D. B. Seidel,
W. Shoup,† W. A. Stygar, and D. H. McDaniel
Sandia National Laboratories
Department 9573, MS-1194
Albuquerque, NM 87185-1194

M. A. Mostrom and K. W. Struve
Mission Research Corporation
1720 Randolph road SE
Albuquerque, NM 87106

P. Corcoran, I. Smith, and P. Spence
Pulse Sciences, Inc.
600 McCormick Avenue
San Leandro, CA 94577

Abstract

Sandia is modifying the PBFA II accelerator into a dual use facility. While maintaining the present ion-beam capability, we are developing a long-pulse, high-current operating mode for magnetically-driven implosions. This option, called PBFA II-Z, will require new water transmission lines, a new insulator stack, and new magnetically-insulated transmission lines (MITLs). Each of the existing 36, coaxial water pulse-forming sections will couple to a 4.5-Ω, bi-plate water-transmission line. The water transmission lines then feed a four-level insulator stack. The insulators are expected to operate at a maximum, spatially-averaged electric field of ~ 100 kV/cm. The MITL design is based on the successful biconic Saturn design. The four "disk" feeds will each have a vacuum impedance of ~ 2.0 Ω. The disk feeds are added in parallel using a double post-hole convolute at a diameter of 15 cm. We predict that the accelerator will deliver 20 MA to a 15-mg z-pinch load in 100 ns, making PBFA II-Z the most powerful z-pinch driver in the world providing a pulsed power and load physics scaling testbed for future 40-80-MA drivers.

Introduction

The PBFA-II accelerator[1] at Sandia National Laboratories, used by the light-ion-beam ICF Program, is being modified to permit dual-use operation. We are making major modifications to the electrical design to optimize coupling of the generator to magnetically-imploded loads, typically z pinches. The layout of PBFA II-Z is seen in Fig. 1.

This paper describes the performance goals, the electrical design constraints and criteria, the modeling, and the predicted performance. PBFA II-Z represents Sandia's first major pulsed-power facility wholly designed using computer-aided drafting (CAD) techniques. It is also the first machine modeled from the wall plug to the load using every known component performance factor. This included detailed 2- and 3-D E&M PIC modeling of the vacuum magnetically-insulated transmission lines (MITLs).

While the overall electrical design of PBFA II-Z is conservative in some aspects it reaches the limits of our understanding. The MITL design is based on our present understanding of magnetic insulation. The coupling of the MITLs to the load through the vacuum post hole convolute is not well understood. Issues such as radiation-driven vacuum gap closure, limits on current density near the load, and vacuum flow in convolutes need to be studied in detail in the future. PBFA II-Z will be able to study some of these fundamental pulsed power concerns while addressing the z-pinch physics necessary for the next generation of drivers.

† Permanent Address: Field Command, Defense Nuclear Agency, Albuquerque NM.

DISCLAIMER

DISCLAIMER

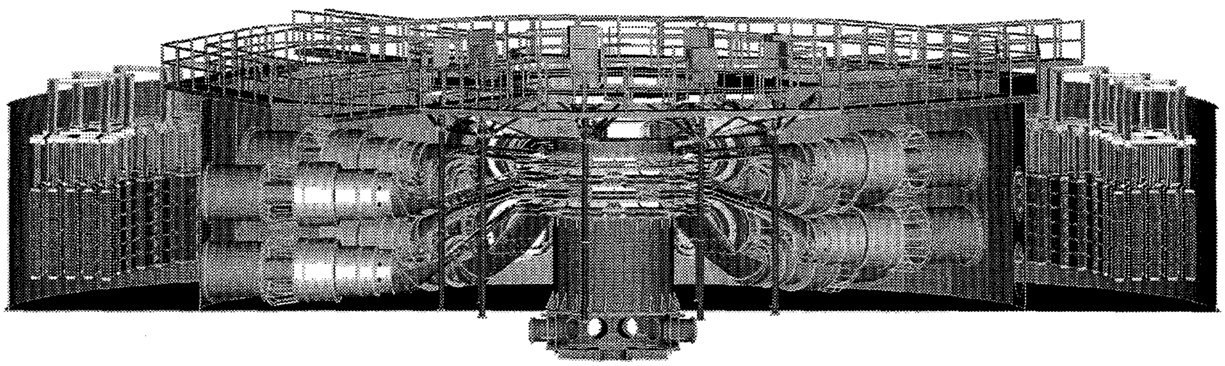

Fig. 1 A schematic of the proposed PBFA II-Z accelerator showing the modifications planned inside the coaxial PFL section.

Performance Requirements and Basic Design Elements

The basic performance specifications for PBFA II-Z were determined by its potential performance (the stored energy) and the desire for the PBFA II-Z accelerator to address critical pulsed power and z-pinch scaling issues for next generation pulsed power facilities.

We established performance goals of 20 MA delivered to a z-pinch load with a rise time of 100 ns, > 1 MJ of x-ray yield, and one shot a day capability. These goals then drove the detailed design of PBFA II-Z. The 20-MA design goal was chosen as a reasonable step to a 40- to 60-MA driver. The 100-ns driving pulse is a tradeoff between the desired short, high-voltage Saturn-like pulse to drives fast implosions and the Rayleigh-Taylor instabilities generated by longer pulse, lower voltage options. The requirement for shot rate is based on the perceived shots needed to get an acceptable learning rate in an R&D environment.

The basic mechanical and pulsed power design of PBFA II-Z was documented earlier in the PBFA II-Z White Paper.[2] We wanted to minimize the cost of the modifications while meeting the performance goals. This resulted in modifying all of the components inside the coaxial pulse-forming lines (PFLs). (See Fig. 1.)

We used Sandia's Screamer[3] and Pulse Sciences' TLCODE[4] transmission-line circuit codesto model possible PBFA II-Z designs using a wide range of electrical parameters such as driving impedance, load inductance, pulse width, and z-pinch mass. We obtained results consistent with our earlier work on generator design. The optimum driving impedance to couple electrical energy to a z-pinch load is roughly set by the time constants of the system, $Z \sim L/\tau$. With a 100-ns driving pulse and a 10-nH inductance we found that the predicted optimum of 0.1 Ω matched the more realistic Screamer prediction of 0.12 Ω quite well. Fig. 2 shows a series of calculations in which the driving impedance is varied while the input energy, inductance, and load mass are held fixed.

Our calculations resulted in the basic electrical and load parameters of the PBFA II-Z design. We need a load driven by ~ 0.1 Ω, a pulse with a rise time of ~ 100 ns, a total vacuum inductance of ~ 10 nH, and a 10 to 15-mg load with a length of ~ 2 cm and radii between 1 and 2 cm. Improvements in kinetic energy delivered to the z-pinch load are determined almost solely by minimizing the inductance of the load, increasing the efficiency of the MITLs, and reducing losses in the vacuum post-hole convolute.

Water Transmission Lines

The PBFA II-Z water lines consist of a transition from the existing co-axial section through bi-plate lines to the insulator stack. The key design issues are to operate in a regime where the lines do not electrically breakdown and to have a constant impedance line.

We used tests of the existing PBFA II water lines to determine the water break down characteristics. These tests used of

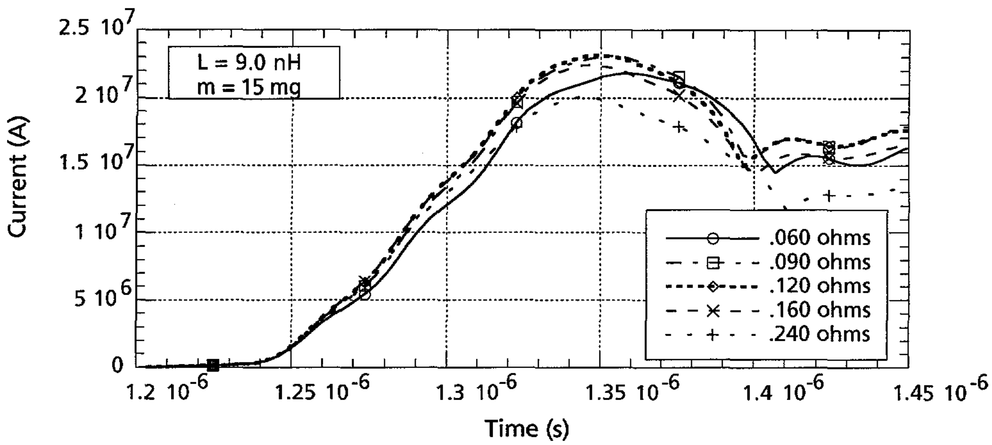

Fig. 2 A plot showing the effect of impedance on the current delivered to a z-pinch load with the input energy held constant.

two PBFA II modules delivering 2.5-MV voltage pulses to simulated PBFA II-Z water transmission lines. In this case we used a 4.5-Ω water line with an 11.4-cm line spacing. The voltage pulse had a 100-ns rise time.

One of the lines was terminated with a resistive load while the other was terminated in an inductive load similar to the expected load of PBFA II-Z. The water lines contained energy damping crowbar features to minimize potential damage to the water lines. In both cases the water lines carried the voltage pulse without arcing although the crowbar switches broke down on the reflected pulse. We concluded that the proposed PBFA II-Z water line design was workable.

We established a baseline water line electrical design of 36, 4.5-Ω water lines having a 14-cm line spacing. The design consisted of a constant impedance transition from coaxial to bi-plate geometry. The length of the bi-plate section was chosen to allow transit-time isolated voltage measurements. Each water transmission line will have a voltage monitor located so that it is transit-time isolated from the insulator stack to provide an accurate forward-going voltage waveform. Fig. 3 shows schematics of the water lines. Using this water line configuration as the working design , we modeled the electric fields throughout the lines looking for edge enhancements and joint effects as well as localized effects due to the superposition of the forward-going voltage pulse and the reflected pulse. Fig. 4 shows the results of electrostatic modeling of the lines. The voltages used in the electrostatic calculations were obtained from the peak voltages calculated in Screamer for that particular position on the water line.

Vacuum Insulator Stack

The existing vacuum insulator stack on PBFA II was designed for light ion experiments. The combined stack consisted of eight separate stacks. It was impossible to design a low inductance MITL and vacuum convolute to utilize such a stack. It was then necessary for us to design a completely new insulator stack.

The decision to design and build a completely new insulator stack was made primarily for inductance reasons. It was critical to have an insulator stack that minimized inductance in order to meet the 20-MA milestone as well as the desired z-pinch kinetic energy. We based our initial PBFA II-Z design on the Saturn insulator stack design. We chose a design consisting of four separate insulator stacks. This was the optimal design for a MITL system based on a double post hole convolute. The 36, water transmission lines were already arranged in four levels of nine lines so it was natural to feed each of the four insulator stacks with nine water transmission lines.

The design of the insulator stack, including the height of the individual insulators, was iterated several times. An initial design was chosen, the inductance calculated, the self-consistent voltage generated with Screamer and the stress across the stack calculated. Based on the insulator flashover criterion (discussed later) the height of the stack was adjusted and the entire process repeated. This resulted in the stack design shown in Fig. 5. We found that the optimal design had five insulators on A and B levels (the levels nearest the load) and six insulators on C and D levels (the

Fig. 3 A schematic of the proposed water transmission lines for PBFA II-Z.

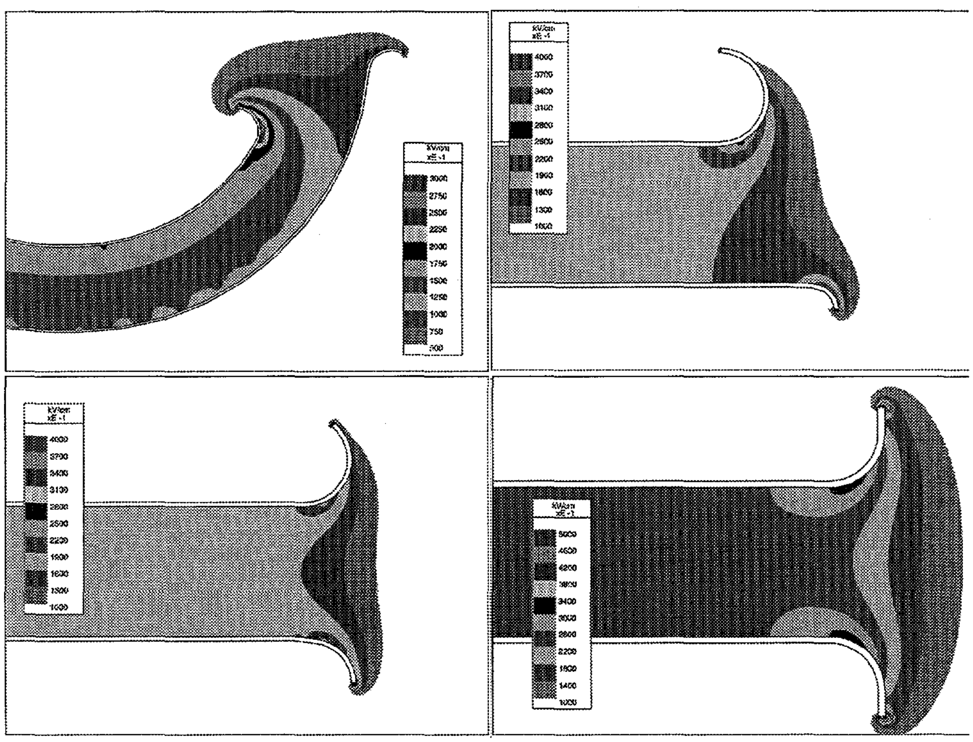

Fig. 4 A plot showing the magnitude of the electric field at four locations in the water lines as the lines convolute from disk to parallel plate. Contours of magnitude of the electric field are plotted for the water lines from the coaxial section to the bi-plate section going from left to right and top to bottom.

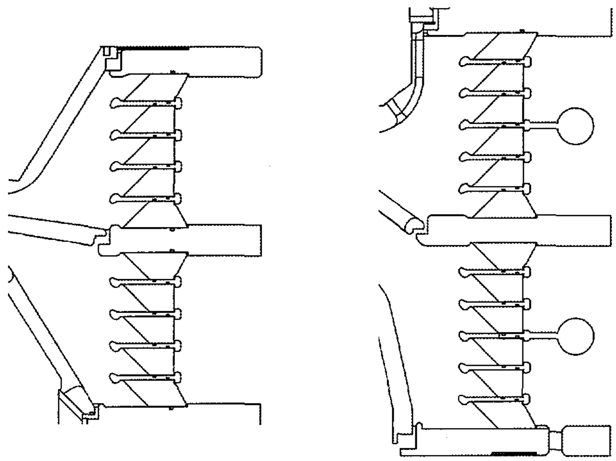

Fig. 5 A schematic showing the details of the A and B level insulator stack (LHS) and the C&D level insulator stack (RHS).

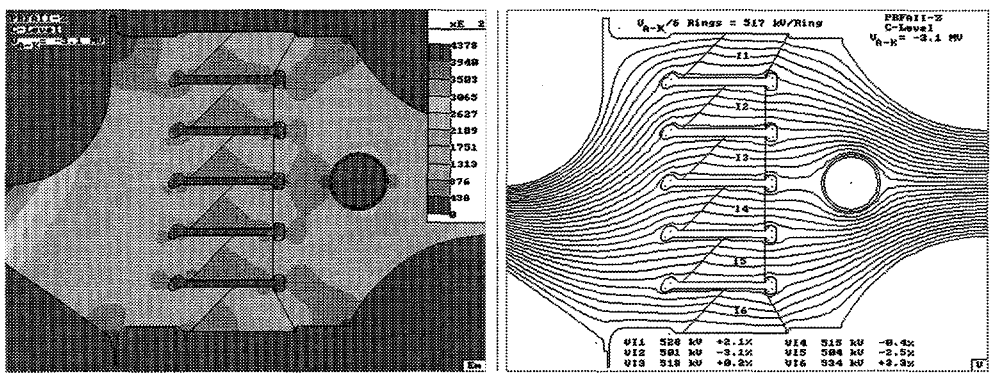

Fig. 6 A plot showing the magnitudes and equipotential contours of the electric field at the insulator on C-Level.

insulators seeing the highest voltage). The actual insulator rings used were nearly identical to PBFA II except that they are to be fabricated from Rexolite™, a cross-linked polystyrene.[5] Rexolite™ is resistant to electron-induced dendrites and has a voltage hold off ~ 14% greater than PMMA. The top modules will have five, 5.72-cm thick and 169-cm outer-radius Rexolite™ insulators. The bottom two modules will have six, similar Rexolite™ insulators. The insulators will have a 45° angle on the vacuum/plastic side.

After the basic insulator stack design was fixed the details of the electric field had to be graded. The grading across individual insulator stacks had a design criterion of ± 5% and was achieved by using flux excluders in the water just outside the insulators on C and D levels and by shaping the conductors near the insulators. An example of the final stack grading is shown in Fig. 6. In this case the average electric field is 90 kV/cm and the grading is ±3.3%.

The insulator stack design utilizes grading rings as part of the overall grading concept. The grading rings have a potential problem of electron emission. In our MITL designs we use re-entrant anode configurations where the large vacuum gap between the anode and the cathode just inside the insulator stack is reduced by having the anode rapidly approach the cathode. This results in a negative potential on the grading rings relative to the nearby anode and the possibility for electron emission if the surface electric field exceeds 250-300 kV/cm. This problem was seen and addressed on Saturn by shaping the grading ring tips. We adopted a similar approach giving the grading ring shape shown in Fig. 7. In the final design we achieved a peak field of 250 kV/cm on the tip of the grading ring. We used IVORY[20] to model the impact of electron emission from grading rings. (See Fig. 8.) In this calculation we used the Screamer calculated voltage waveform to drive a design identical to our final design - except the grading ring to

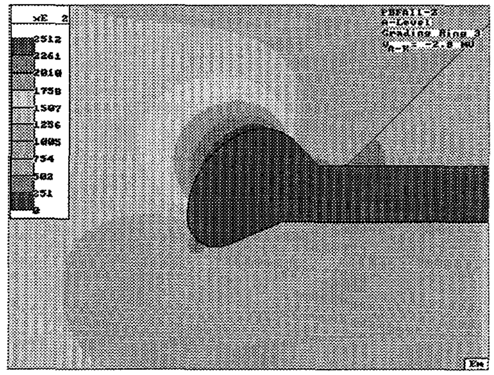

Fig. 7 A plot showing the grading ring tip and the magnitude of the electric fields on A-level, grading ring #3.

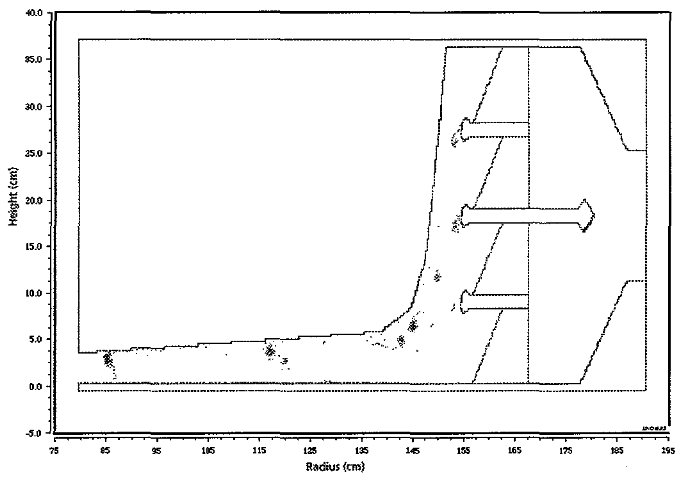

Fig. 8 A diagram showing the details of electron emission from the grading ring tips.

anode distance was halved to force field emission of electrons. These calculations showed that emission from the grading rings changes the ±3% grading of the insulator stack to +51%/-38%, essentially ruining the stack grading.

One major concern for the PBFA II-Z insulator stack design was insulator break down. The data base assembled by J. Charlie Martin and coworkers[6] has limited applicability to the very large insulator areas and stack diameters found on the PBFA II-Z multi-insulator stack. The standard insulator breakdown formula (the so-called JCM limit),

$$Ft^{1/6}A^{1/10} = 175,$$

makes significant area and time scaling assumptions when applied to the PBFA II-Z stack. A re-analysis of J. Charlie Martin's data shows that a time dependence as strong as $t^{1/4}$ is not unreasonable. Statistically, we expect the area term to become weaker for large area insulator stacks. Additionally, the JCM limit does not address the effect of multiple insulator tubes. One of us (I. Smith) has modified J. Charlie Martin's formula to include a stronger time dependence and a statistical probability for stack breakdown when there are multiple insulators per stack. (See the paper by Ian Smith in these Proceedings.) We also used existing Saturn data and PBFA II data to examine experimental operating limits for insulator break down. A synthesis of the existing data and the scaling relations has resulted in our prediction that the proposed PBFA II-Z stack design would operate very near the breakdown limits but should work without breakdown in 9 out of 10 shots.

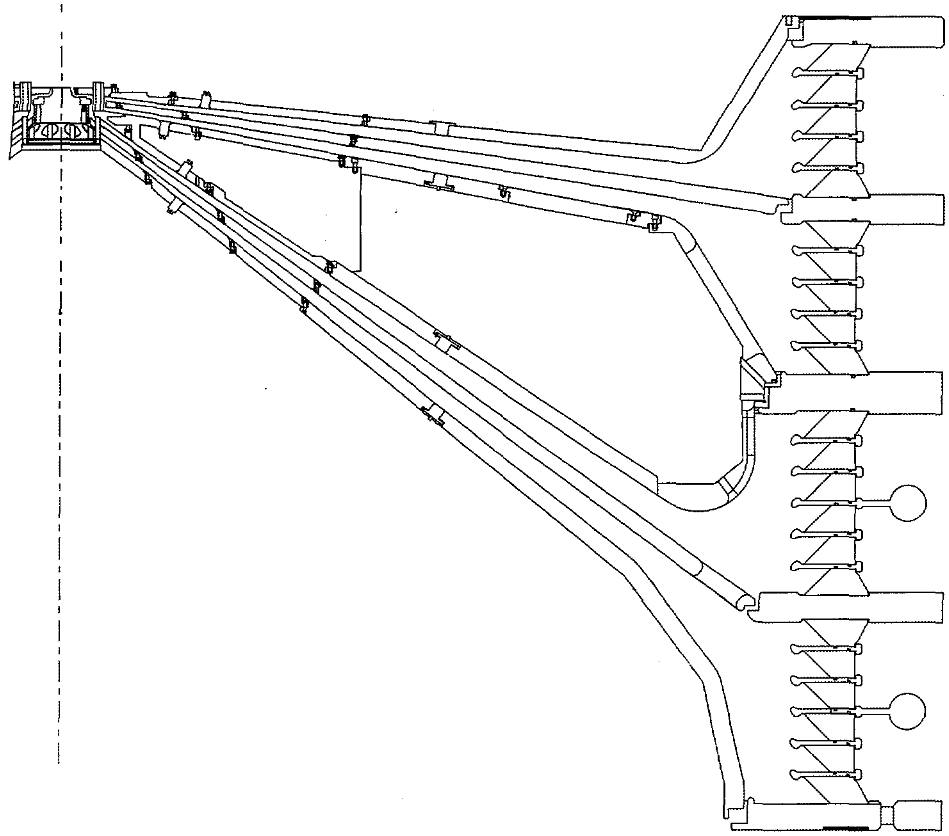

Fig. 9 A picture of the proposed MITLs for PBFA II-Z showing the transition from the insulator stack to the post-hole convolute.

The insulator stack will contain voltage and current monitors on each level. This will enable an accurate measurement of the electrical performance of the stack, MITLs, and load. We will be able to carefully compare the measured forward-going voltage with the voltage measured at the insulator stack. These data will allow a accurate comparison of the machine performance with Screamer and TLCODE predictions.

Vacuum Magnetically-Insulated Transmission Lines and Convolute

The design of the PBFA II-Z vacuum section is outlined in Figure 9. The four axisymmetric MITLs shown in the Figure are joined in parallel at a 7.6-cm radius by a double post-hole convolute.[7] Downstream of the convolute a single 5-cm-long MITL feeds power to the load. The design is based on the successful PROTO-II[8] and Saturn[9] vacuum sections. This minimizes risk, and allows the continuation of a 15-year power-flow-scaling experiment: four-level MITL-convolute configurations were tested at 5 and 10 MA on PROTO II and Saturn, respectively, and will be evaluated at 20 MA on PBFA II-Z.

The MITL-gap profiles are tri-linear functions of radius. The impedance profiles minimize the fraction of the total current carried by the electron-sheath, with the constraint that at least 20 MA be delivered to the baseline 2-cm-long, 2-cm-initial-radius, 15-mg-mass load. The gap profiles limit the electron dose to the anode to $\leq$ 50 J/g, which is less than the 150 J/g and 300 J/g thresholds required for anode-plasma formation in stainless steel and aluminum, respectively.[10-13] The design accounts for a 2.5 cm/μs cathode-plasma expansion velocity.[14-17] For the baseline load, the initial inductance inside the stack-vacuum interface is 10 nH.

The MITL design was developed with iterative TLCODE,[4] SCREAMER,[3] TRIFL,[18] TWOQUICK,[19] IVORY,[20] and 1-D LASNEX[21] simulations. Various aspects of the design were investigated with the different computational tools. TRIFL is a new 1-D MITL simulation code, TWOQUICK and IVORY are 2-D electromagnetic particle-in-cell codes, and LASNEX is a magneto-hydrodynamic code with radiation transport. Results from a typical TWOQUICK

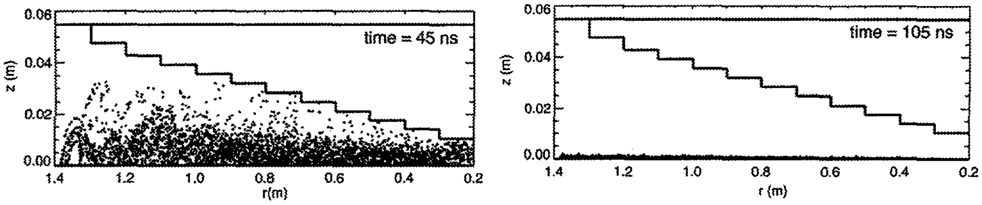

Fig. 10 TWO-QUICK calculations showing the establishment of magnetic insulation in PBFA II-Z MITLs. This calculation includes the dynamic impedance effect of the z-pinch load.

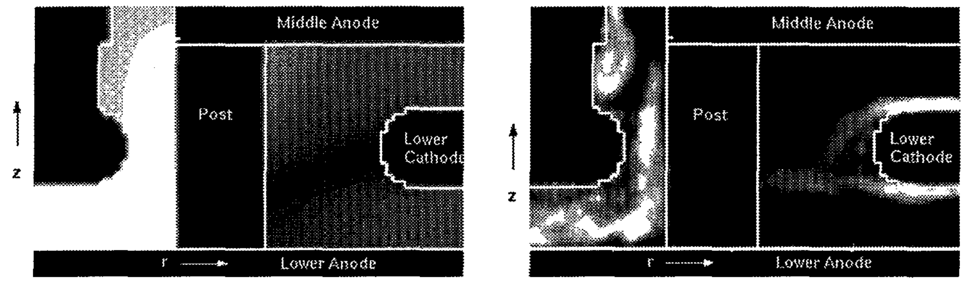

Fig. 11 QUICKSILVER calculations showing contours of the magnitude of the magnetic field and electron flow off the cathode following the magnetic null between a cathode hole and an anode post.

simulation are shown in Figure 10, and show that vacuum electron flow fills the MITL anode-cathode gap early in time but near peak current becomes well trapped and forms a thin sheath near the cathode. The currents predicted by the codes agreed to within 4%.

The double-post-hole convolute, an inherently three-dimensional device with magnetic nulls at current bifurcations, was modeled with QUICKSILVER,[22] a 3-D electromagnetic particle-in-cell code. (Please see Figure 11.) Results indicate that, to a very good approximation, all of the electron-sheath current launched in the MITLs upstream of the convolute is lost at the magnetic nulls, and that at peak current the intrinsic efficiency of the convolute is essentially 100%. These results are valid only for loads with the characteristic low impedance of z-pinches.

MITL B-dot current monitors will be located at three radial locations: in all four outer disk MITLs at an 80-cm radius, in all four outer disk MITLs just upstream of the convolute, and in the inner disk MITL. We will also use piezoelectric current probes, located at a 3-cm radius, to measure the total current delivered to the z-pinch load. The MITL diagnostic package will be used to improve the understanding of MITL performance, vacuum-convolute losses, and power flow in high-current-density regions. The MITL-stack interface has been designed to permit changing the MITL AK gaps +1.0/-1.2 cm in support of the power-flow experiments.

The MITL electrodes are being fabricated from stainless steel and aluminum. These materials are readily available, have low outgassing rates, and have low physical-surface areas.[23-26] Stainless will be used for the MITL cathodes to provide uniform electron emission.[27] Stainless will be used for the MITL anodes for radii $\leq$ 70 cm - where gaps are the smallest - because the higher mass density will provide a longer component lifetime. The MITL anodes will be aluminum at larger radii to keep the total weight $\leq$ 9 tons for single-step loading with the overhead PBFA-II crane.

The mechanical design of the MITLs has been validated with NISA[28] and ALGOR[29] finite-element modeling.

Conclusion

PBFA II-Z is an accelerator for z-pinch implosion experiments that is designed to deliver 20 MA to the load. The conservative design philosophy focused on pulsed power reliability although provisions have been made for power flow studies. We have used the latest pulsed power data in establishing the overall design criteria.

PBFA II-Z will extend our knowledge base for pulsed power in water power flow, insulator stack voltage hold off, MITL behavior and electron flow, and vacuum convolutes.

Acknowledgements

The authors would like to thank the invaluable assistance of a large number contributors, throughout government and industry, without whose pulse power expertise this work would have been impossible. The rapid development and many iterations of the PBFA II-Z design would not have been possible without the unstinting efforts of the Sandia Engineering and Drafting organizations.

*This work was supported by the U.S. Department of Energy under Contract #DE-AC04-94AL85000.

References

[1] B. N. Turman, et al., *Proc. Of the Fifth IEEE Pulsed Power Conf.*, Arlington, VA 1985, pp. 155.
[2] R. B. Spielman, "PBFA II-Z White Paper", Internal Sandia Memorandum, June 1994.
[3] M. L. Kiefer, K. L. Fugelso, K. W. Struve, M. M. Widner, SCREAMER, A Pulsed Power Design Tool, 25 August 1995 (Sandia Internal Document).
[4] W. N. Weseloh, *Proc. Of the Seventh IEEE Pulsed Power Conf.*, Monterey, CA 1989, pp. 989.
[5] O. Milton, *IEEE Transactions on Electrical Insulation* Ei-7, #1 March 1972, pp. 9.
[6] J. C. Martin, Fast Pulse Vacuum Flashover, SSWA/JCM/713/157 and AFWL High Voltage Notes, Note 2, 16 March 1971.
[7] R. B. Spielman, P. Corcoran, J. Fockler, H. Kishi, and P. W. Spence, in *Proceedings of the 7th IEEE International Pulsed Power Conference* (1989), p. 445.
[8] T. H. Martin, J. P. VanDevender, D. L. Johnson, D. H. McDaniel, and M. Aker, in *Proceedings of the International Topical Conference on Electron Beam Research and Technology*, Albuquerque, NM, 1976, Vol. 1, p. 450 .
[9] D. D. Bloomquist, et al., *Proc. of the Sixth IEEE Pulsed Power Conf.*, Arlington, VA edited by P. J. Turchi and B. H. Bernstein (IEEE, New York, 1987), p. 310.
[10] T. W. L. Sanford, et al., Sandia Laboratory Report SAND88-1297 (1988).
[11] P. Spence, K. Triebes, R. Genuario, and D. Pellinen, in *Proceedings of the International Topical Conference on Electron Beam Research and Technology*, Albuquerque, NM, 1976, Vol. 1, p. 346.
[12] A. E. Blaugrund, G. Cooperstein, S. A. Goldstein, Phys. Fluids, 20, 1185 (1977).
[13] M. E. Cuneo, R. M. Gilgenbach, and M. L. Brake, *IEEE Trans. on Plasma Science*, PS-15, 4 (1987).
[14] G. A. Mesyats and D. I. Proskurovsky, *Pulsed Electrical Discharge in Vacuum*, (Springer-Verlag, New York, 1988) p. 118-120.
[15] R. K. Parker, Richard E. Anderson, and Charles V. Duncan, J. Appl. Phys. 45, 2463 (1974).
[16] R. W. Stinnett, M. A. Palmer, R. B. Spielman, and R. Bengston, *IEEE Trans. on Plasma Science*, PS-11, 216 (1983).
[17] V. G. Kovalev, et al., Sov. Phys. Tech. Phys. 37, 813 (1992).
[18] C. W. Mendel (private communication).
[19] T. D. Pointon, J. Comput. Phys. **96**, 143 (1991).
[20] M. M. Campbell, B. B. Godfrey, and D. J. Sullivan, Mission Research Corporation Report AMRC-R-454, 1988 revised.
[21] P. D. Nielsen, Ph. D. Thesis, University of California, 1981 (Report UCRL-53166) and R. Humphreys (private communication).
[22] D. B. Seidel, et al., *1991 Proc. Of the CP90 Europhysics Conf. On Computational Physics*, A. Tenner, ed., (World Scientific, Singapore), pp. 475-482 and J. P. Quintenz, D. B. Seidel, M. L. Keifer, T. D. Pointon, R. S. Coats, Se. E. Rosenthal, T. A. Mehlhorn, M. P. Desjarlais, and N. A. Krall, Laser and Particle Beams **12**, 283 (1994).
[23] John F. O'Hanlon, A User's Guide to Vacuum Technology (John Wiley and Sons, New York, 1989).
[24] J. Blears, E. J. Greer, and J. Nightingale, in *Proceedings of the 1st International Congress on Vacuum Technology*, 1958, Advances in Vac. Sci. Technol. vol. 2, p.473 (1960).
[25] A. Roth, Vacuum Technology (North-Holland, New York, 1982).
[26] L. Holland, W. Steckelmacher, J. Yarwood, *Vacuum Manual* (E. & F. N. Spon, London, 1974).
[27] D. H. McDaniel, private communication.
[28] Engineering Mechanics Research Co., P. O. Box 696, Troy, Michigan 48099.
[29] ALGOR Inc., 150 Beta Dr., Pittsburgh, PA 15238.